Cell Reports, Volume *28*

Supplemental Information

Drp1 Promotes KRas-Driven Metabolic Changes to Drive Pancreatic Tumor Growth

Sarbajeet Nagdas, Jennifer A. Kashatus, Aldo Nascimento, Syed S. Hussain, Riley E. Trainor, Sarah R. Pollock, Sara J. Adair, Alex D. Michaels, Hiromi Sesaki, Edward B. Stelow, Todd W. Bauer, and David F. Kashatus

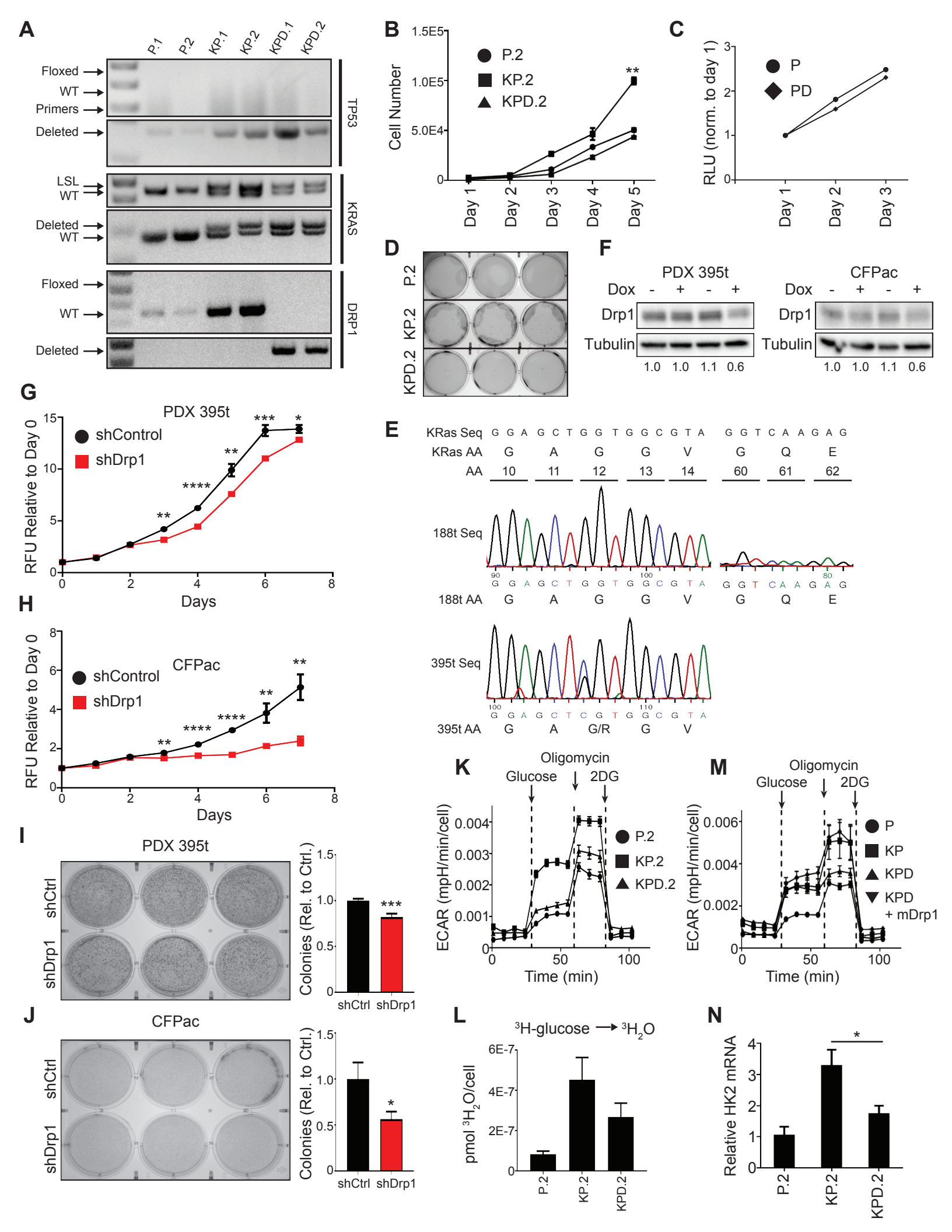
A
P.1
P.2
KP.1
KP.2
KPD.1
KPD.2
Floxed
WT
Primers
Deleted
TP53
LSL
WT
Deleted
WT
KRAS
Floxed
WT
Deleted
DRP1
B
Cell Number
1.5E5
1.0E5
5.0E4
0
P.2
KP.2
KPD.2
**
Day 1
Day 2
Day 3
Day 4
Day 5
C
RLU (norm. to day 1)
P
PD
Day 1
Day 2
Day 3
D
P.2
KP.2
KPD.2
F
PDX 395t
Dox - + - +
Drp1
Tubulin
1.0 1.0 1.1 0.6
CFPac
Dox - + - +
Drp1
Tubulin
1.0 1.0 1.1 0.6
G
PDX 395t
shControl
shDrp1
RFU Relative to Day 0
Days
H
CFPac
shControl
shDrp1
RFU Relative to Day 0
Days
E
KRas Seq G G A G C T G G T G G C G T A G G T C A A G A G
KRas AA G A G G V G Q E
AA 10 11 12 13 14 60 61 62
188t Seq
188t AA G A G G V G Q E
395t Seq
395t AA G A G/R G V
I
PDX 395t
shCtrl
shDrp1
Colonies (Rel. to Ctrl.)
shCtrl shDrp1
J
CFPac
shCtrl
shDrp1
Colonies (Rel. to Ctrl.)
shCtrl shDrp1
K
Oligomycin
Glucose
2DG
ECAR (mpH/min/cell)
P.2
KP.2
KPD.2
Time (min)
M
Oligomycin
Glucose
2DG
ECAR (mpH/min/cell)
P
KP
KPD
KPD + mDrp1
Time (min)
L
3H-glucose → 3H2O
pmol 3H2O/cell
P.2
KP.2
KPD.2
N
Relative HK2 mRNA
P.2
KP.2
KPD.2

Figure S1: Drp1 contributes to KRas-driven cellular transformation. Related to Figures 1-3. A. PCR to determine the genotype and recombination status of p53, KRas, and Drp1 of the indicated MEFs. **B.** The indicated cell lines were seeded at equal density and cells were counted daily over a five-day period (n=3 replicates per cell line, representative result from one of three independent experiments, mean ± SEM, **P<0.01, one-way ANOVA with Tukey's multiple comparison). **C**. The indicated cell lines were seeded at equal density and cells were quantified over a three-day period using CellTiter Glo. **D.** Equal numbers of the indicated cells lines were seeded in soft agar and imaged after 3 weeks (n=3). **E**. PCR amplification and sequencing were performed for a portion of the KRAS gene (exon 2, 3) in PDX 188t and PDX 395t. **F.** Immunoblot analysis of Drp1 in indicated human pancreatic cancer cell lines with doxycycline inducible shRNA against Drp1. Doxycycline = 2 µg/mL. Quantification of densitometry relative to shCtrl cells with no doxycycline below blot (Tubulin = loading control). **G, H.** The PDX395t cell line (**G**) and CFPac cell line (**H**) were seeded at equal density in media containing 2 µg/mL doxycycline and cells were analyzed by CyQuant over a 7 day period with regular media changes (n=3 replicates per cell line, 3 independent experiments, data presented as mean ± SEM, *P<0.05, **P<0.01, **** P<0.001, ****P<0.0001, unpaired two-sided Student's T–test). **H, I.** Equal numbers of the PDX 395t (**I**) and CFPac (**J**) cells lines were seeded in soft agar, then stained and imaged after 2 weeks. Quantification for number of colonies > 0.01 mm^2 relative to shCtrl (n=3 replicates per cell line, 3 independent experiments, * P<0.05, ***P<0.001, unpaired two-sided Student's T–test. Data are mean ± SEM) **K.** Extracellular acidification rate (ECAR) was analyzed on the indicated MEF lines over a 100 minute time course of a Glycolysis Stress Test. Glucose, oligomycin and 2-DG were added at the indicated time points (n=3 replicates per cell line, data presented as mean ± SEM, representative result from one of three independent experiments). **L.** Equal numbers of the indicated MEFs were seeded and incubated in Glycolysis Stress Test media. A bolus of 10mM glucose with ^{3}H-Glucose was added and incubated for 1 hour and the production of ^3H_2O was analyzed as a readout of glycolytic flux (n=3 replicates per cell line, 3 independent experiments, one-way ANOVA with Tukey's multiple comparison. Data are mean ± SEM). **M.** Extracellular acidification rate (ECAR) was analyzed on the indicated MEF lines over a 100 minute time course of a Glycolysis Stress Test. Glucose, oligomycin and 2-DG were added at the indicated time points (n=3 replicates per cell line, data presented as mean ± SEM, representative result from one of three independent experiments). **N.** Real-time qPCR analysis of relative HK2 mRNA levels in the indicated MEFs (n=3 replicates per cell line, 3 independent experiments, data are aggregate means ± SEM, *P<0.05, **P<0.01, one-way ANOVA with Tukey's multiple comparison).

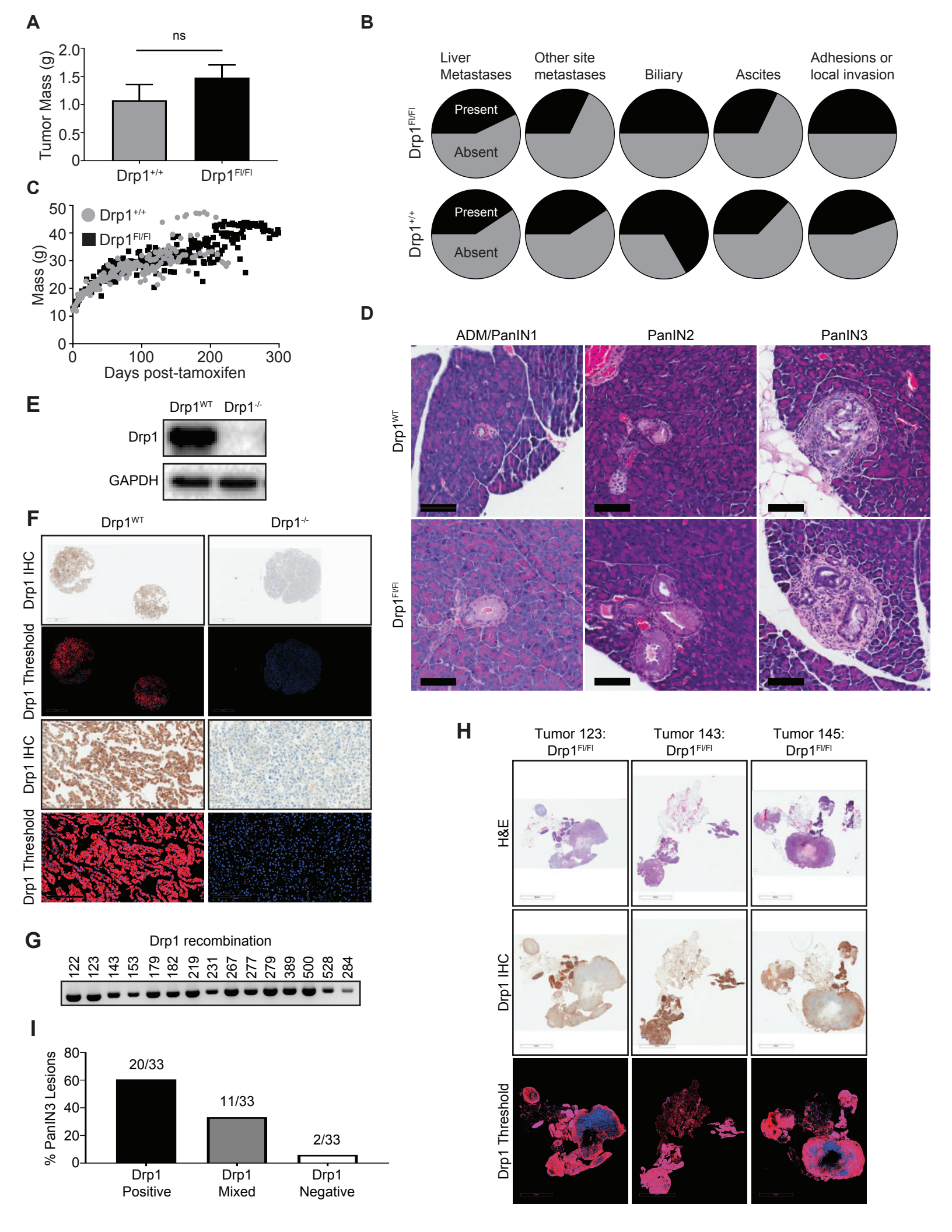
A
ns
Tumor Mass (g)
2.0
1.5
1.0
0.5
0
Drp1+/+
Drp1Fl/Fl
B
Liver Metastases
Other site metastases
Biliary
Ascites
Adhesions or local invasion
Drp1Fl/Fl
Present
Absent
Drp1+/+
Present
Absent
C
Drp1+/+
Drp1Fl/Fl
Mass (g)
50
40
30
20
10
0
0
100
200
300
Days post-tamoxifen
D
ADM/PanIN1
PanIN2
PanIN3
Drp1WT
Drp1Fl/Fl
E
Drp1WT
Drp1-/-
Drp1
GAPDH
F
Drp1WT
Drp1-/-
Drp1 IHC
Drp1 Threshold
Drp1 IHC
Drp1 Threshold
G
Drp1 recombination
122
123
143
153
179
182
219
231
267
277
279
389
500
528
284
H
Tumor 123: Drp1Fl/Fl
Tumor 143: Drp1Fl/Fl
Tumor 145: Drp1Fl/Fl
H&E
Drp1 IHC
Drp1 Threshold
I
% PanIN3 Lesions
80
60
40
20
0
20/33
11/33
2/33
Drp1 Positive
Drp1 Mixed
Drp1 Negative

Figure S2: Comparison of tumor sequelae and Drp1 expression in Drp1^{Flox} and Drp1^{WT} mice. Related to Figure 4. A. Tumors were isolated from *Kras*$^{LSL\text{-}G12D/+}$; *Trp53*$^{flox/flox}$; *Drp1*^{WT}; *Pdx-1-CreER*$^{Tg/+}$ mice and *Kras*$^{LSL\text{-}G12D/+}$; *Trp53*$^{flox/flox}$; *Drp1*$^{flox/flox}$; *Pdx-1-CreER*$^{Tg/+}$ mice and tumor weights were determined at necropsy (n=18 Drp1^{WT}, n=12 Drp1^{flox}, Data are mean ± SEM, n.s. = P>0.05, Student's T-test). **B.** The presence or absence of the indicated tumor sequelae was evaluated for the indicated sets of mice at necropsy (n=27 Drp1WT, n=28 Drp1flox). **C.** Enrolled mice were weighed 3X per week following tamoxifen injections until survival endpoints were reached. Data presented as weight trajectories as a function of time (n=30 Drp1^{WT} and Drp1^{flox}). **D.** Pancreata were removed from *Kras*$^{LSL\text{-}G12D/+}$; *Trp53*$^{flox/flox}$; *Drp1*^{WT}; *Pdx-1-CreER*$^{Tg/+}$ mice and *Kras*$^{LSL\text{-}G12D/+}$; *Trp53*$^{flox/flox}$; *Drp1*$^{flox/flox}$; *Pdx-1-CreER*$^{Tg/+}$ mice at 40 or 60 days following tamoxifen injection. Tissue was fixed and stained with H&E to examine the incidence of the indicated pancreatic lesions. Scale bars, 100 μm. **E.** Immunoblot analysis of Drp1 expression in the Drp1^{WT} and Drp1$^{-/-}$ MEFs. GAPDH = loading control. **F.** Cell pellets of Drp1^{WT} and Drp1$^{-/-}$ MEFs in **E** were paraffin-embedded and Drp1 expression was analyzed by immunohistochemistry (IHC). Low magnification Drp1 IHC images of cell pellet (top row) with corresponding color deconvoluted image (2nd row). High magnification Drp1 IHC images of cell pellet (3rd row) with corresponding color deconvoluted image (4th row). **G.** Cre-mediated recombination at the Drp1 locus was analyzed in DNA from pancreatic tumors isolated from Drp1^{flox} mice. **H.** Tumors isolated from Drp1^{flox} mice at necropsy were stained with hematoxylin & eosin (H&E; top row), Drp1 IHC (2nd row), and corresponding color deconvoluted image (3rd row). **I.** Drp1 expression was analyzed by IHC in PanIN3 lesions from Drp1^{flox} mice euthanized 60 days after tamoxifen injection. Lesions in which all morphologically attributable epithelial cells express Drp1 were scored as positive. Lesions in which some, but not all, morphologically attributable epithelial cells within a lesion express Drp1 were scored mixed. Lesions in which no morphologically attributable epithelial cells within a lesion express Drp1 were scored negative.

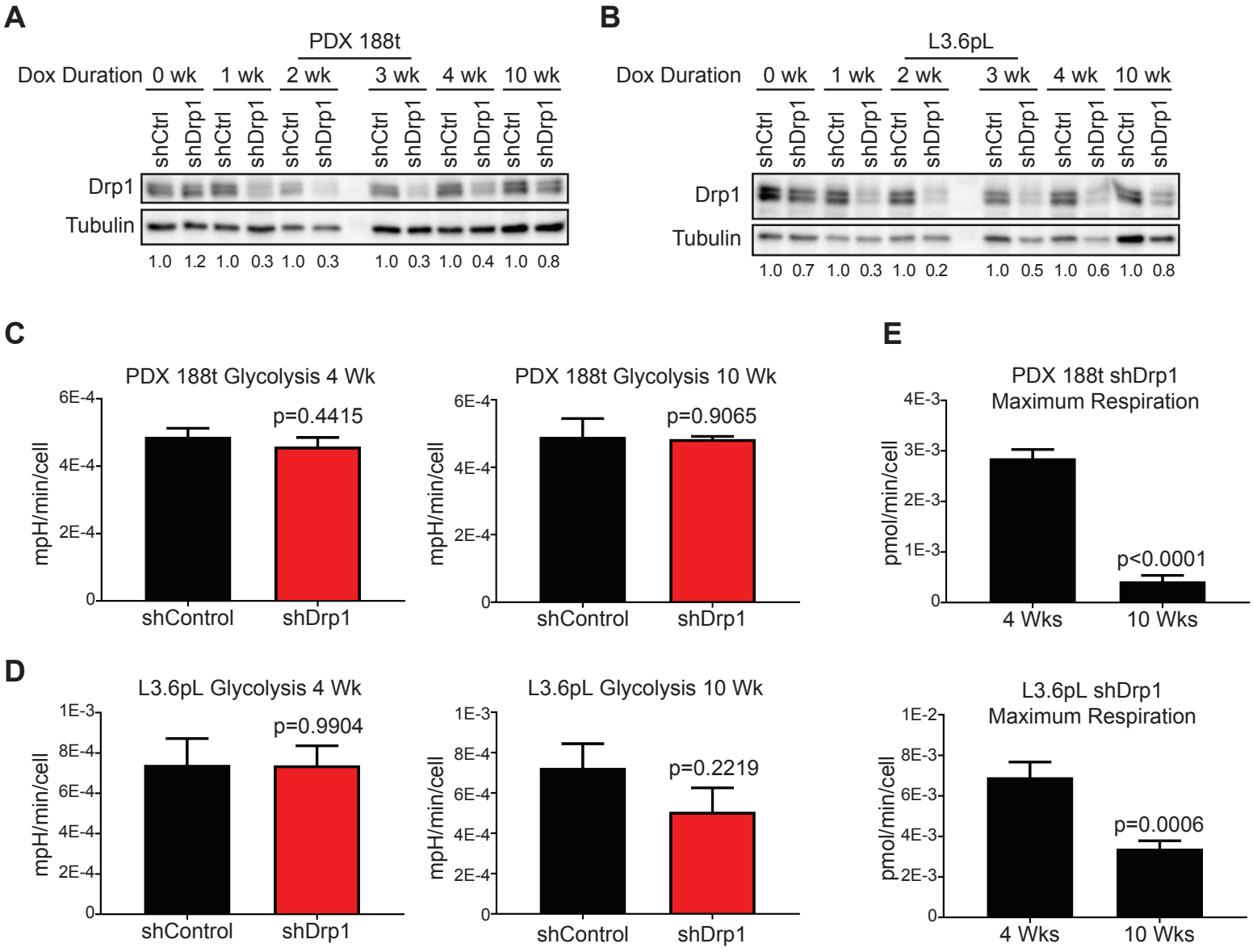

Figure S3. Increased duration of Drp1 knockdown alters the bioenergetic profile in human pancreatic cancer cell lines. Related to Figures 5 & 6. A, B. Immunoblot analysis of Drp1 in PDX 188t (**A**) and L3.6pL (**B**) cell lines with doxycycline inducible shRNA against Drp1. Doxycycline dosage was 2 µg/mL. Quantification of densitometry relative to shCtrl cells with no doxycycline provided below blot (Tubulin = loading control). **C, D**. ECAR was analyzed on the PDX 188t (**C**) and L3.6pL (**D**) cell lines after 4 weeks (left panel) and 10 weeks (right panel) of doxycycline treatment over a 120-minute time course during a Glycolysis Stress Test and used to calculate ECAR attributable to glycolysis (n=2-3 replicates per cell line, 3 independent experiments, unpaired two-sided Student's T–test. Data are mean ± SEM). **E**. OCR was analyzed on the indicated human pancreatic cancer cell lines cell lines after 4 weeks and 10 weeks of doxycycline treatment over a 120-minute time course during a Mitochondrial Stress Test and used to calculate OCR attributable to maximal respiration (n=2-3 replicates per cell line, 3 independent experiments, unpaired two-sided Student's T–test. Data are mean ± SEM).

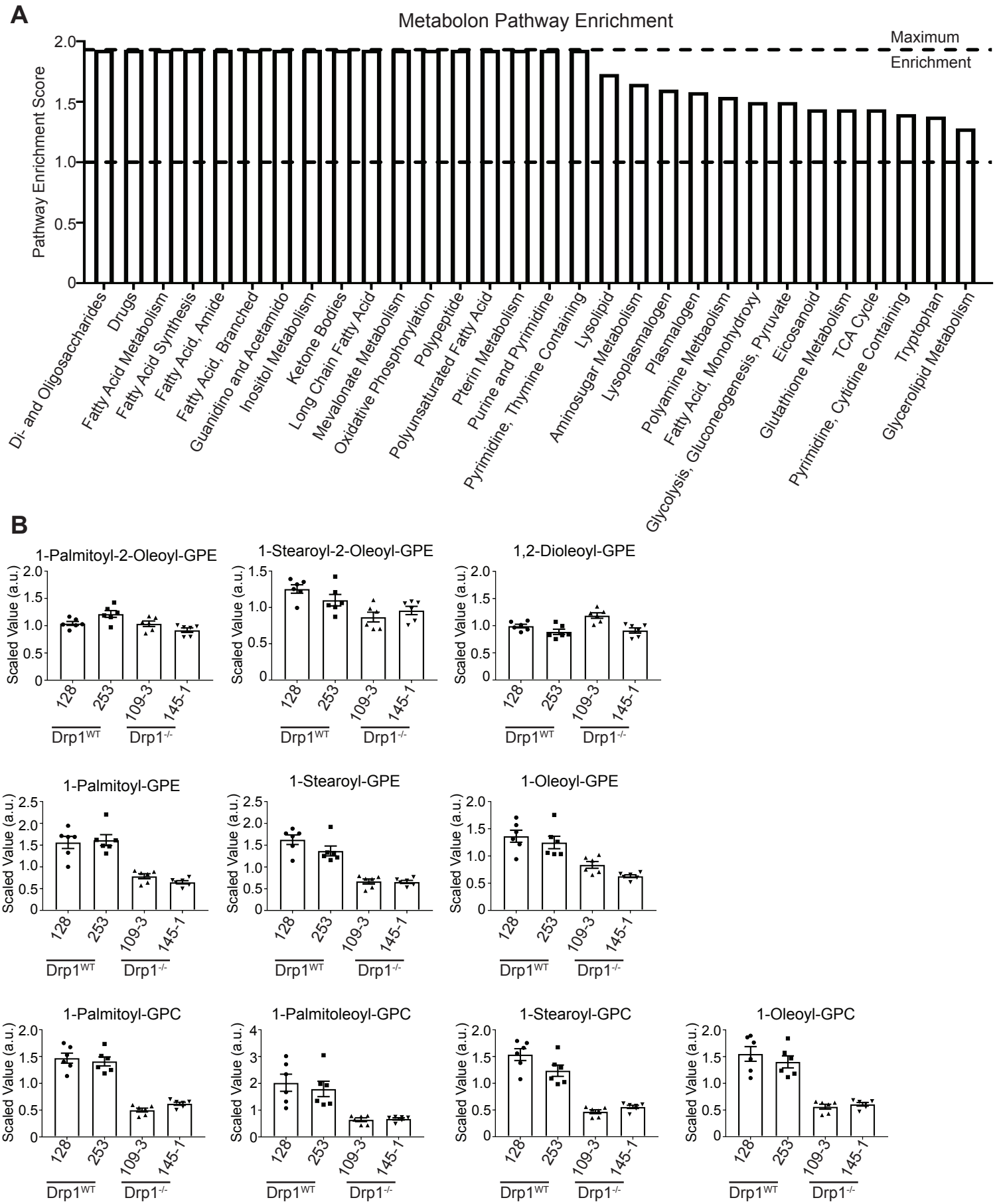

Figure S4: Drp1-/- tumor cells exhibit metabolic reprogramming. Related to Figures 5 & 6. A. Pathway enrichment analysis was performed on 350 metabolites that were significantly different between the pairwise comparison of all Drp1$^{-/-}$ and Drp1^{WT} tumor-derived cell lines to identify potential metabolic pathways dependent on Drp1. **B.** The scaled abundance of three phosphatidylethanolamine (PE) species (top row), the corresponding lyso-PE species (second row), and the lyso-PC corresponding to the PC species in Figure 6F (third row) from metabolomic analysis of the indicated Drp1^{WT} and Drp1$^{-/-}$ tumor-derived cell lines (n=6 replicates per cell type, data are mean ± SEM).

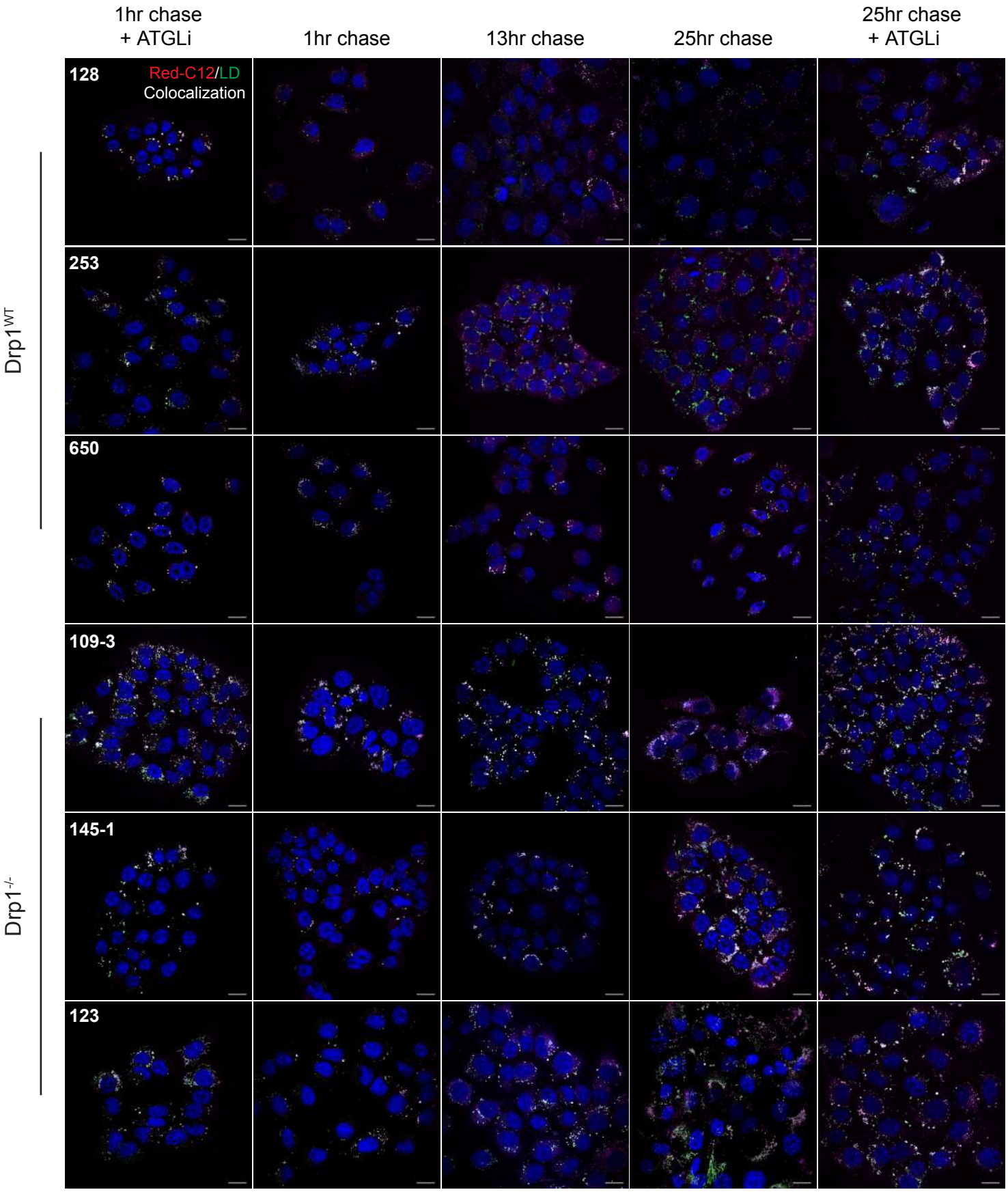

Figure S5. Fatty acids efflux from lipid droplets more rapidly in Drp1^{WT} tumor cells compared to Drp1$^{-/-}$ tumor cells. Related to Figure 7. Representative images of a panel of Drp1^{WT} (top 3 rows) and Drp1$^{-/-}$ (bottom 3 rows) tumor cells were pulsed with Red C12 (fatty acids, magenta) for 12 hours in DMEM supplemented with 10% FBS and chased in DMEM supplemented with 10% FBS for 25 hours. Cells at the indicated time points were fixed and stained with BODIPY 493/503 (lipid droplets, green) and DAPI (nuclei, blue). Where indicated, Atglistatin, an ATGL inhibitor, was added for the duration of the pulse and chase.

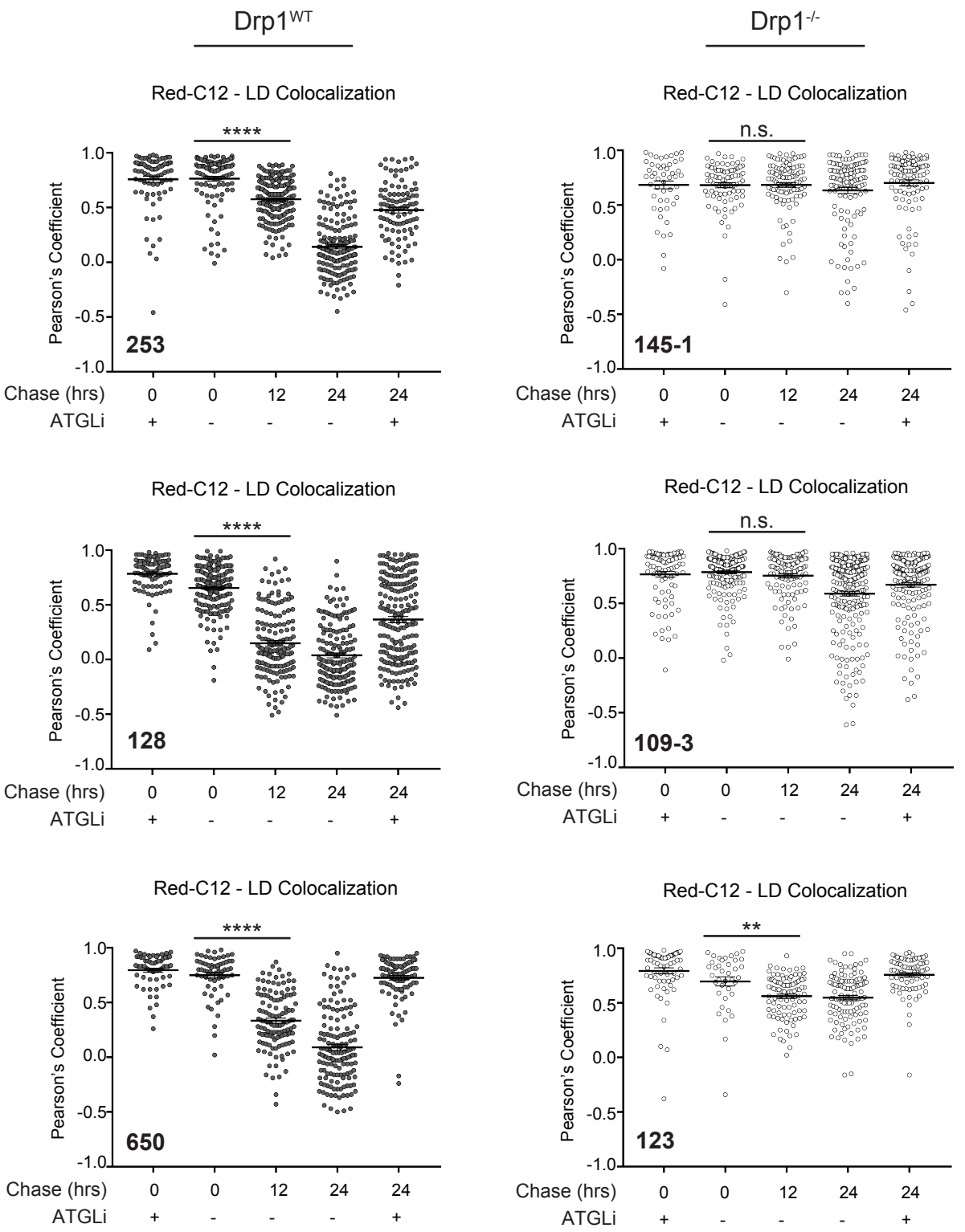

Figure S6. Fatty acids efflux from lipid droplets more rapidly in Drp1^{WT} tumor cells compared to Drp1$^{-/-}$ tumor cells. Related to Figure 7. Quantification of images for each cell line from Supplementary Figure S5. Each data point represents the Pearson's correlation coefficient between RedC12 and BODIPY for each cell (n=3 independent experiments for 128 and 109-3 cell lines and n=2 independent experiments for remaining cell lines, ≥ 50 cells were analyzed for each time point of each cell line, data are means ± SEM, *P<0.05, ** P< 0.01, *** P<0.001, ****P < 0.0001, one-way ANOVA with Tukey's multiple comparison)

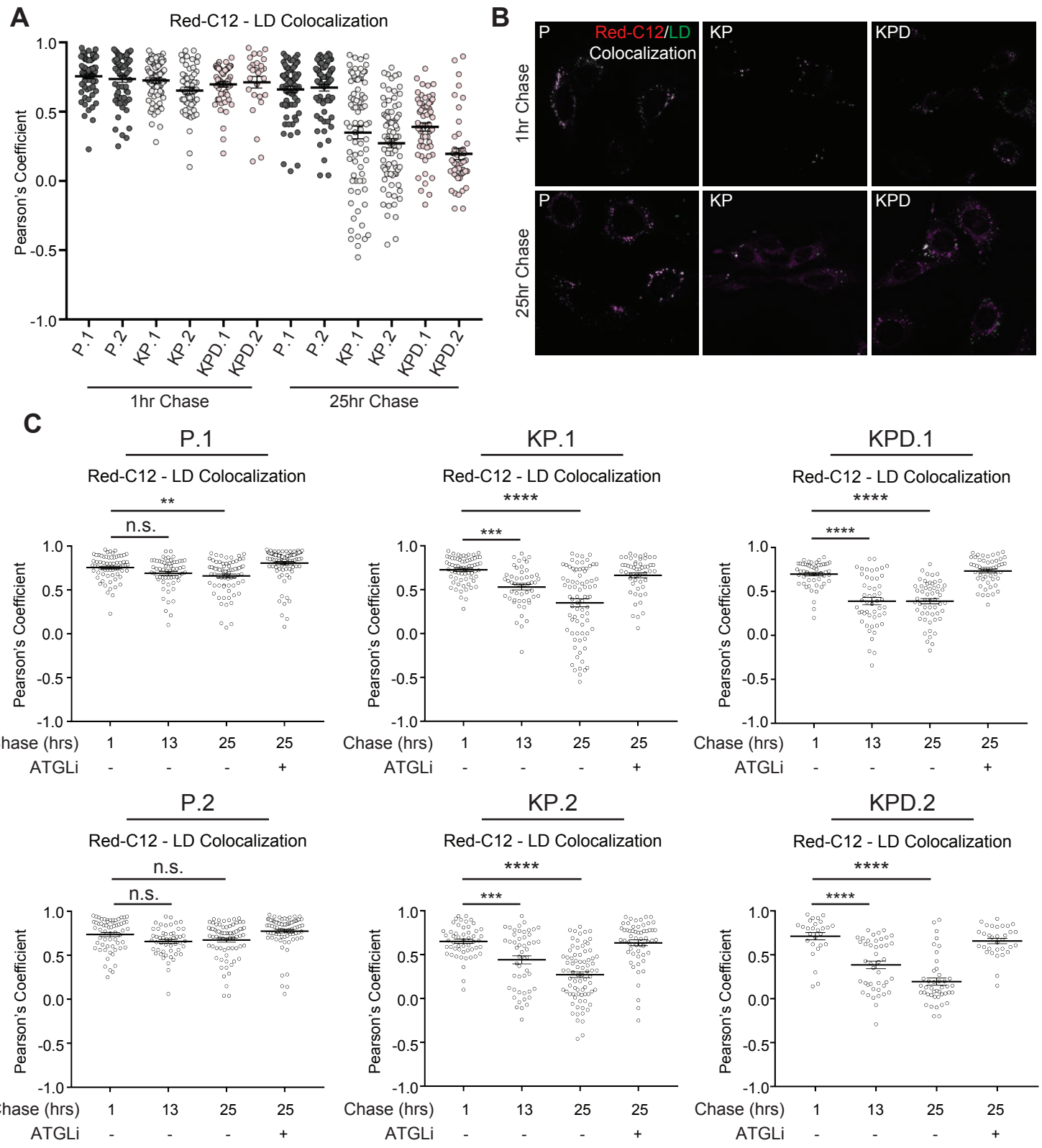

Figure S7. KRas-induced fatty acid efflux from lipid droplets in MEFs does not require Drp1. Related to Figure 7. The indicated MEFs were were pulsed with Red-C12 (fatty acids, magenta) for 12 hours in DMEM + 10% FBS and chased in DMEM without Red-C12 for 25 hours. Cells were fixed and stained with BODIPY493/503 (lipid droplets, green). Where indicated, Atglistatin, an ATGL inhibitor, was added for the duration of the pulse-chase. **A**. Quantification after 1 and 25 hours. Each point represents the Pearson's correlation coefficient between RedC12 and BODIPY for one cell (n=3 independent experiments, ≥50 cells per time point per cell line, data are means ± SEM,*P<0.05, ** P< 0.01, *** P<0.001, ****P < 0.0001, one-way ANOVA with Tukey's multiple comparison). **B.** Representative images. Scale bars, 20μm. **C.** Identical analysis as A but expanded for each indicated MEF for 1, 13, 25 hours of chase as well as 25 hours + ATGLi.